Development of Planar, Shape-changing Rigid Body Segmentation Process for General Design Profiles

S. A. Shamsudin[*1,3], Z. Zainal[2,3], M. N. Sudin[1,3], H. A. Al-Issa[4]

[1] Centre for Advanced Research on Energy (CARe), Universiti Teknikal Malaysia Melaka, 75450 Ayer Keroh, Melaka, Malaysia

[2] Centre for Robotics and Industrial Automation (CeRIA), Universiti Teknikal Malaysia Melaka, 76100 Durian Tunggal, Melaka, Malaysia

[3] Fakulti Kejuruteraan Mekanikal (Faculty of Mechanical Engineering), Universiti Teknikal Malaysia Melaka, 75450 Ayer Keroh, Melaka, Malaysia

[4] Department Electrical and Electronics Engineering, AlBalqa Applied University, As-Salt, Jordan

ABSTRACT

This work describes the early segmentation results in the progress of a mechanism design process to produce simple planar machines that could approximate a shape change defined by a set of curves with significant differences in arc length. The design profiles vary from one another by a combination of rigid-body displacement and shape change that includes significant differences in arc length. Where previous rigid-body shape-change work focused on mechanisms composed of rigid links and revolute joints to approximate curves of roughly equal arc length, this work introduces prismatic joints into the mechanisms in order to produce the different desired arc lengths. The first step is to convert the design profiles into piecewise linear curves, referred to as target profiles. The piecewise linear representation that proves most useful has points identified along the curve at roughly equal distances. The second step is to compare segments of the target profiles seeking those that are best approximated by a common rigid body and those that share curvature similarities allowing for the introduction of a prismatic joint. In the end, implementing the procedure in MATLAB could create a chain of rigid bodies that are joined by revolute and prismatic joints. The chain can closely estimate the shape of a set of design profiles.

KEYWORDS: Shape-change, mechanisms, kinematic synthesis, planar

1.0   INTRODUCTION

Some machines like aircraft wings, for instance, rely on their ability to fluctuate between specific shapes in a pre-determined way. For instance, evaluate the usefulness of diverse wing airfoils for cruising as opposed to active dog-fighting situations. Many military agencies are always exploring for a better technology that will enable wings to actively shift shapes to achieve wide variety of flight characteristics as well as surface control, which might be impossible with the state-of-the-art wings (Weishaar, 2006). The rewards from such a shape-changing mechanism that can morph among specified profiles and then

hold-on to the shapes is noteworthy. Meanwhile, others like (Lu & Kota, 2003) applied some optimization algorithms for discrete topology in compliant mechanisms for shifting the shapes of parabola antennas.

Many methods can be used to achieve a morphing capacity such as compliant mechanisms and memory alloy materials as described in literature like (Trease, Moon & Kota, 2005), (Lateş, Căşvean & Moica, 2017) and (Rubbert et al., 2017). Besides these, there are also works with shape-memory alloys that can be actuated by electrical signals or heat such as by (Lobo, Almeida & Guerreiro, 2015), (Mohd Jani et al., 2013), and (Nespoli et al., 2010). Concerns with these methods include practical cost and limited displacement size. Shape-changing rigid body mechanisms have been proposed as an alternate to the above technologies to achieve the range of displacement needed from a rigid-body linkage mechanism with a well-established set of mechanical design principles (Korte, 2006).

Consequently, the rigid-body shape-changing mechanisms use the concept of breaking up the curves into segments. Each segment is optimized in shape and length so that it can best approximate the same portion on each target profile. Figure 1 depicts the outcome of such segmentation process. The shape of each segment is basically the mean shape of that portion. Researchers in (Murray, Schmiedeler & Korte, 2008) suggested adding up binary links to each segment in order to connect the segment to fixed pivots while achieving lower degree-of-freedom when the system change shapes.

The presently available synthesis methods for designing shape-changing rigid-body mechanisms better address problems with profiles of roughly the same arc length. This is a serious limitation of the current methodology. Hence, this paper includes developments to the theory that introduce prismatic joints into the chain of bodies used to approximate design profiles.

This paper presents the segmentation methodology for profiles with significant differences in arc length that are expected to include prismatic joints in their mechanized form. First, design profiles are converted into target profiles. Then, the curvatures of the profiles are compared to allow for the introduction of a prismatic joint. Finally, the remaining segments of the design curves are approximated with rigid bodies connected by revolute joints.

2.0   METHOD

A design profile is a curve defined by (Murray, Schmiedeler & Korte, 2008) such that an ordered set of points on the curve and the arc length between any two such points can be determined. In earlier rigid-body shape-change work, design profiles were converted into piecewise linear target profiles where each target profile contained the same number of points. When the curves were assumed to be of roughly equal arc length, this distribution of points resulted in curves where each piecewise linear segment is roughly equal in length. Given that the curves may now possess large differences in arc length, representation of different design profiles by the same number of points could produce individual linear segments of considerably different length.

The length of segment in a piecewise linear curve is

$$S_i = \sqrt{(x_{i+1} - x_i)^2 + (y_{i+1} - y_i)^2}, \quad i = 1, \dots n - 1 \qquad (1)$$

Note that i is the point number on the profile curve. The total length of the curve is then

$$L_j = \sum_{i=1}^{n-1} S_i \qquad (2)$$

Note that j is the curve number on the profile set. Given that we seek to represent a curve by desired segments of length S_d,

$$m_j = L_j / S_d \qquad (3)$$

Hence, we get the first guess at the number of points that needs to be on the curve as shown in Equation (4). The m_j number of segments is actually rounded down to make errors on the side too short.

$$n_j = m_{a_j} + 1 \qquad (4)$$

Equation (2) shows that as all the segment length S_i where i = 2, 3, 4... N, the last point on the curve. However, in Equations (3) and (4), the new number of segments m_j and new number of points n_j are determined. These numbers must be integer.

The next step is to distribute the n points (which are n_j of that profile curve) equidistantly along the curve. Then, this new attribute of the curve is reviewed. Manipulating Equation (3), check the segment length. Basically, this is refinement step aimed at getting the segment length as close as possible to the desired segment length. The result is the actual segment length as shown in Equation (5).

$$S_{a_j} = L_j / m_{a_j} \qquad (5)$$

Actually, to get the actual segment length as close as possible to the desired segment length, we increase or decrease the number of points n by 1 as we compare S_{a_j} and S_d. Figure 1(a) shows the part in the software being developed, that manipulate the segment length in all the curves in concern. On the other hand, in Figure 1(b), the points have been redistributed by segment length. The desired segment length here is 3 units. As a result, the number of points also changes in both the curves in order to get as close as possible to that desired value.

3.0   CURVATURE CALCULATIONS

With the 3 data points, the curvature of the middle point (j[th] point) is calculated. This will mean the first data point and the last one cannot have their curvature calculated as such since these points are not in the middle of the first or the last 3 points. However, the first point will assume the curvature of the second point the last point (N[th] point) will assume that which is before it i.e. (N-1) [th] point.

It is known that the curve can be approximated by circles of various radii. The radius of each circle is conversely proportional to its curvature. Thus, the curvature is

$$\kappa = 1/r \tag{6}$$

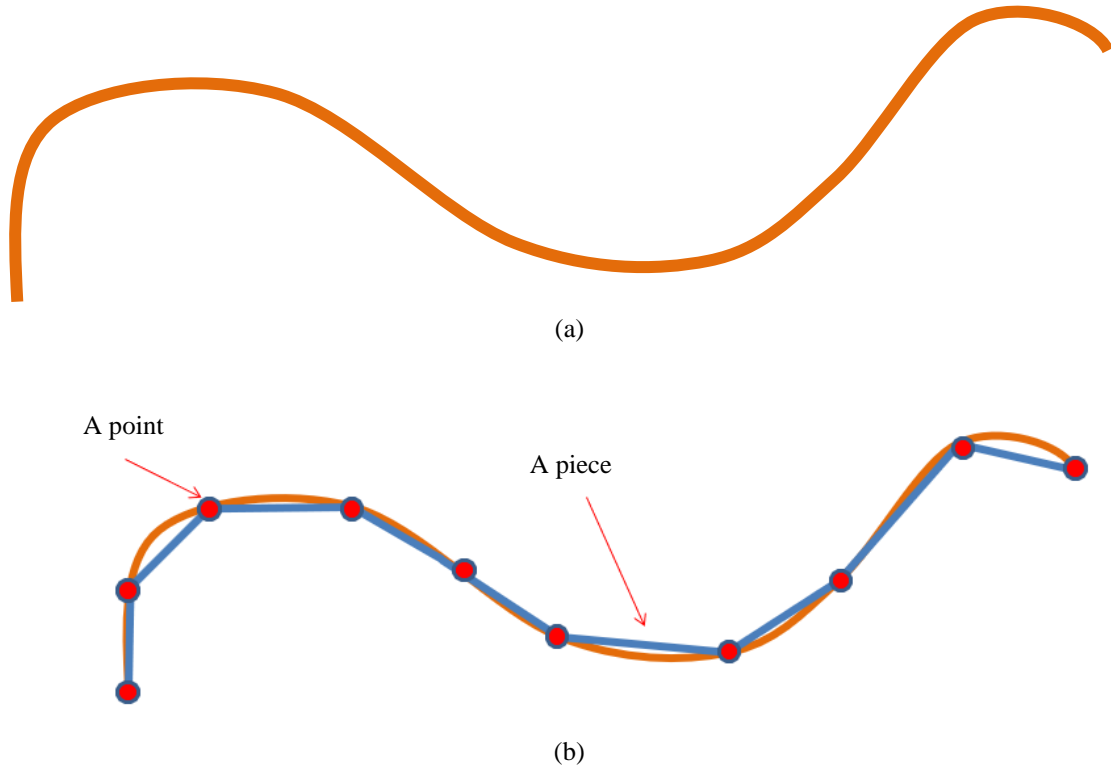and the center point for the circle is (a, b).

(a)

(b)

Figure 1. (a) This shows a continuous design profile. (b) This shows a target profile curve with 9 pieces at a certain average piece length shown with two points per piece. The smaller mean piece length of the target profiles seems to approximate well the shape of the design profiles.

The curvature will also have sign that is positive or negative. The polarity is determined by considering the vectors formed by the 3 points considered at a time. Take points 1, 2, and 3 to be represented by $\{x_1, y_1\}$, $\{x_2, y_2\}$, and $\{x_3, y_3\}$ respectively. Then, take the two direction vectors P_1 and P_2 as

$$\mathbf{P_1} = \begin{Bmatrix} x_2 - x_1 \\ y_2 - y_1 \end{Bmatrix} = \begin{Bmatrix} dx_1 \\ dy_1 \end{Bmatrix}$$
$$\mathbf{P_2} = \begin{Bmatrix} x_3 - x_2 \\ y_3 - y_2 \end{Bmatrix} = \begin{Bmatrix} dx_2 \\ dy_2 \end{Bmatrix}$$

Hence the cross product becomes

$$\mathbf{CP} = \mathbf{P_1} \times \mathbf{P_2} = (dx_1 dy_2 - dy_1 dx_2)\boldsymbol{k} \tag{7}$$

If the magnitude $CP = |CP|$ is negative, the curvature κ also becomes negative. Another term that can be derived is the angle θ between the vectors P_1 and P_2. Next, the dot product must be calculated as shown by Equation (8).

$$DP = \mathbf{P_1} \cdot \mathbf{P_2} = (dx_1 dx_2 + dy_1 dy_2) \tag{8}$$

Since $P_1 \times P_2 = |P_1||P_2| \sin\theta$ and $P_1 \cdot P_2 = |P_1||P_2| \cos\theta$, it follows that

$$\theta = \tan^{-1}(|\mathbf{P_1} \times \mathbf{P_2}|/(P_1 \cdot \mathbf{P_2})) \tag{9}$$

The curvature distribution in its original form possesses lots of spikes especially as the curvature is changing signs. The conditions of the spikes depend on how smooth each curve is. To assist on selecting the points for each prismatic joint, the curvature plot might need to be smoothened. However, doing so will also change the corresponding profiles. The user then will have to decide whether the resulting changes to the profiles are acceptable or not.

Murray, Schmiedeler, and Korte (2008) described vividly of a concept to rotate and translate a curve to another curve provided they both have the same number of points. Shamsudin and Murray (2013) even expanded the idea to also include a scaling factor. However, in the rigid body shape-changing case, the scaling is seldom used. If there is a set of p design profiles, let the jth target profile be defined by $z_{j_i} = \{x_j \quad y_j\}^T$, $i = 1, \dots, n$.

$$\mathbf{Z_{j_i}} = \mathbf{A}z_{j_i} + \mathbf{d} \tag{10}$$

where the rotational matrix and translational vector are defined as

$$\mathbf{A} = \begin{bmatrix} \cos\theta & -\sin\theta \\ \sin\theta & \cos\theta \end{bmatrix} \tag{11}$$

and

$$\mathbf{d} = \begin{Bmatrix} d_1 \\ d_2 \end{Bmatrix} \tag{12}$$

Equation (10) can be manipulated to achieve optimum conditions that result in

$$\mathbf{d} = \frac{1}{n}\left(z_{k_T} - Az_{j_T}\right) \tag{13}$$

where it is defined that
$$\mathbf{z_{j_T}} = \sum_{i=1}^{n} z_{j_i} = \{x_{j_T} \quad y_{j_T}\}^T \tag{14}$$

The rotation angle θ for $\mathbf{A}$ can be calculated as

$$Num = (1/n)\left(x_{k_T}y_{j_T} - x_{j_T}y_{k_T}\right) - \sum_{i=1}^{n}\left(x_{k_T}y_{j_T} - x_{j_T}y_{k_T}\right) \tag{15a}$$

$$Den = \sum_{i=1}^{n}\left(x_{j_i}x_{k_i} - y_{j_i}y_{k_i}\right) - (1/n)\left(x_{j_T}x_{k_T} - y_{j_T}y_{k_T}\right) \tag{15b}$$

$$\theta = \tan^{-1}(Num/Den) \tag{15c}$$

Now, with θ and $\mathbf{d}$ known, the profile particular j profile can be shifted to the k profile.
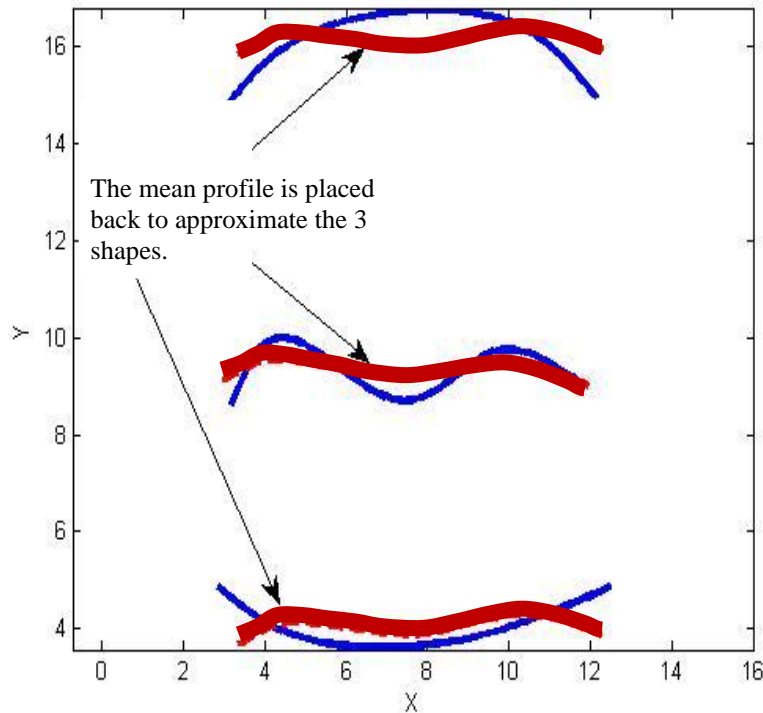
Figure 2. The mean profile is shown here in thick lines brought back in optimized position to each design profile.

Mean segment was explained in detail by (Korte, 2006) and the concept is shown in Figure 2, where a mean profile tries to approximate the three different shapes. Corresponding section of profiles that have same number of points can be shifted together using the minimized distance algorithm and then the mean profile of the section can be generated by

$$z_{m_i} = \frac{1}{p}\left(z_{1_i} - \Sigma_{j=2}^{p} z_{j_i}\right) \tag{16}$$

where $i = 1, \ldots, n$.

All profiles that share the same number of points can be rotated and translated to a fixed profile, say target profile 1. Then from each point, using Equation (16), the mean segment or profile can be generated. Figure 2 also shows that the one mean profile is optimally positioned back to the 3 profiles. Furthermore, the concept of error E is also useful where the maximum value of the point-to-point distances is calculated as the mean profile is placed back to the design profiles. This error reading can be used for further manipulations.

4.0 CURVATURE MANIPULATION

Oftentimes, the curvature distributions from the curves are filled with spikes. Direct calculation of a curvature from 3 points at a time may probably lead to that. However, the curvature values can be manipulated with a scheme, and the resulting new curvature can be used to regenerate the geometric curve it now represents. Should the regenerated curve be still close to the original profile curve, then data from the curvature distribution

can be used for further operations.

The scheme that is suggested here is shown in Equations (17) through (19)

$$\tilde{\kappa}_1 = (2/3)\kappa_1 + (1/3)\kappa_2 \tag{17}$$

and for middle points, the new curvatures become

$$\tilde{\kappa}_i = (1/4)\kappa_{i-1} + (1/2)\kappa_i + (1/4)\kappa_{i+1} \tag{18}$$

where i = 2,3,4, …, N-1, then

$$\tilde{\kappa}_N = (2/3)\kappa_N + (1/3)\kappa_{N-1} \tag{19}$$

The simple example shown in Figures 3 and 4 is meant to show that the smoothing of the curvature plot enables us to see the trend of the plot better. The plot has less spikes and their magnitudes are somewhat reduced anyway.
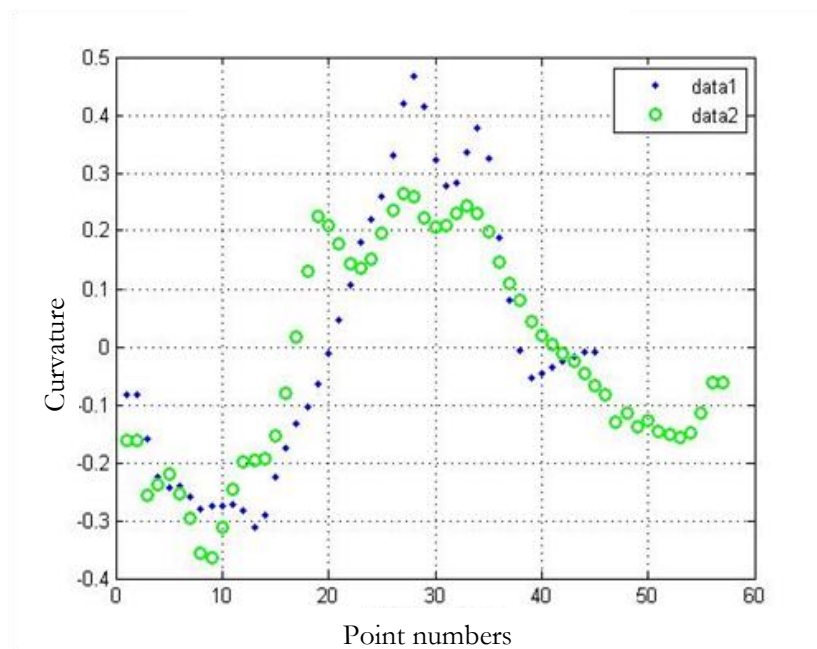

Figure 3. This plot shows the distribution of original curvature data for each profile curve. Profiles 1 and 2 correspond to data 1 and data 2, respectively.
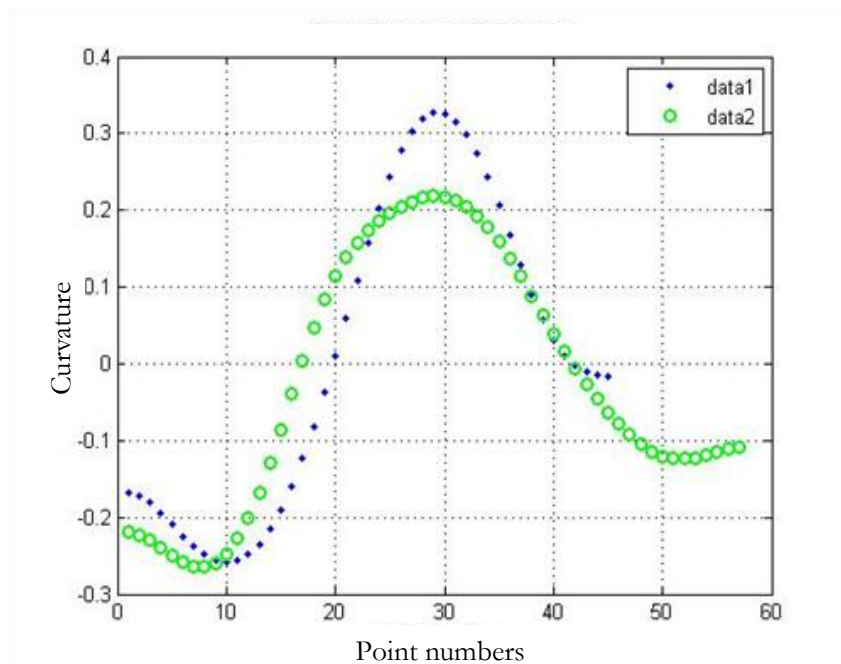
Figure 4. This shows curvature distribution that was smoothened 25 times in order to better see the trend of the distribution. Again, profiles 1 and 2 correspond to data 1 and data 2, respectively.

The application of the smoothing techniques is shown to the same example can be shown as a function of how many times the curvature data is smoothened. Figure 5 below shows the changes in the generated target profiles as compared to the original ones as the curvature distribution changes. The target profiles match the shapes of the design profiles almost perfectly as evident in Figure 6.
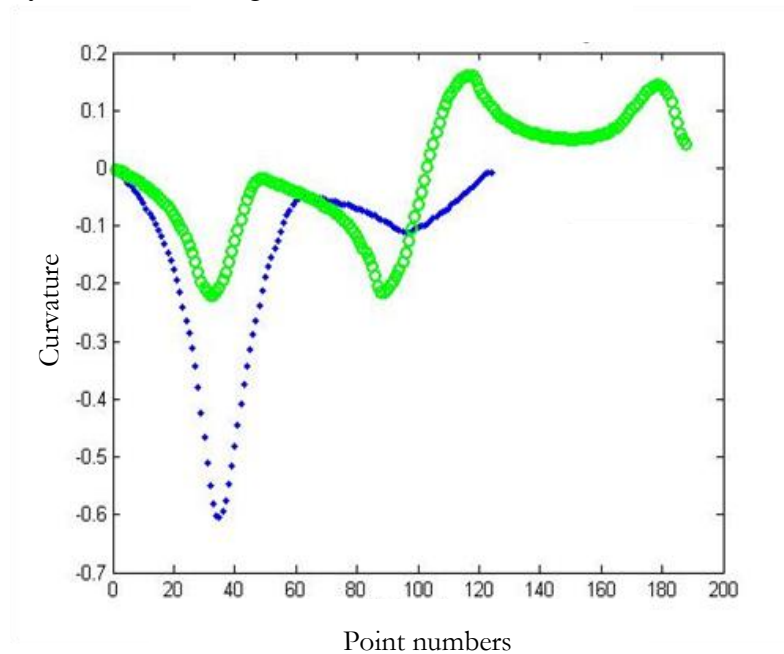
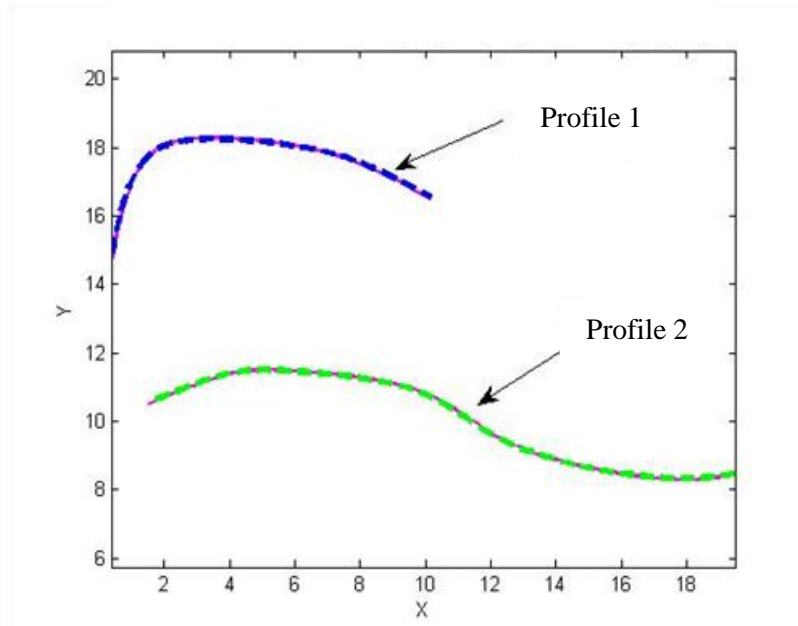

Figure 5. The curvature distribution after smoothing.

Figure 6. The curves plotted after 5 times of smoothing processing.

The user of this system has the ability to choose how much compromise is acceptable based on the differences between profiles that are generated from curvature data and the original profiles. A smoother distribution of curvature can definitely assist in selecting the regions suitable for prismatic joints. If Figure 6(b) is selected as the curvature plot, then in the next process, it will be easier for the user of the system to select the start and end points where a prismatic link will be placed.

The regenerated target profiles were made from information of the curvature. To do this, we refer again to the Equation used to find the curvature. However, now the curvature $\tilde{\kappa}$ is already known from Equation (17) through Equation (19) while the unknowns are the center point (a, b) and the third point (x_3, y_3). The first part is to solve for the center point (a, b) by knowing (x_1, y_1) and (x_2, y_2).

$$(a^2 + b^2) - 2ax - 2by = (r^2 - x^2 - y^2) \tag{20}$$

This Equation (20) can be expanded in matrix form as

$$\begin{bmatrix} 1 & -2x_1 \\ 1 & -2x_2 \end{bmatrix} \begin{Bmatrix} a \\ a^2 + b^2 \end{Bmatrix} + \begin{Bmatrix} 2y_1 \\ 2y_2 \end{Bmatrix} = \begin{Bmatrix} r^2 - x_1^2 - y_1^2 \\ r^2 - x_2^2 - y_2^2 \end{Bmatrix} \tag{21}$$

Now, having center (a, b) from Equation (21), one can solve for (x_3, y_3). Having these coordinates, the profile could then be redrawn from a fixed frame. Once this is done, the method of shifted profiles is applied so that the regenerated profile is shifted back to the original target profile.

One of the ways to find (x_3, y_3) is by using the circle Equation (22) shown below.

$$2ax + 2by + (r^2 - a^2 - b^2) = (x^2 + y^2) \tag{22}$$

This can also be shown in a matrix form as

$$\begin{bmatrix} 1 & 2x_1 & 2y_1 \\ 1 & 2x_2 & 2y_2 \\ 1 & 2x_3 & 2y_3 \end{bmatrix} \begin{Bmatrix} r^2 - a^2 - b^2 \\ a \\ b \end{Bmatrix} = \begin{Bmatrix} x_1{}^2 + y_1{}^2 \\ x_2{}^2 + y_2{}^2 \\ x_3{}^2 + y_3{}^2 \end{Bmatrix} \tag{23}$$

Equation (23) solves for the curvature where curvature is $\kappa = 1/r$ as in Equation (6). However, if the distance between points 1 and 2 is not the same as the distance between points 2 and 3, then when we use data points 1 and 2 as well as the signed value of the curvature of point 2, we can have a choice of 4 possible points for (x_3, y_3).

Nevertheless, since the construction of the target profiles uses finite numbers of roughly equal length segments, then 2 of these possible points coincide with point 1. The other 2 possibilities will have either positive or negative curvature value. The algorithm created should compare these values to match the input curvature value used. This could be from the original data or after the curvature was smoothened.

Figure 7 shows the detection of (x_3, y_3) when the segment lengths are different and another when they are about the same. Normally, the algorithm created would choose the correct point 3. Thus, it is a reliable way to find a unique point 3 in the geometry.
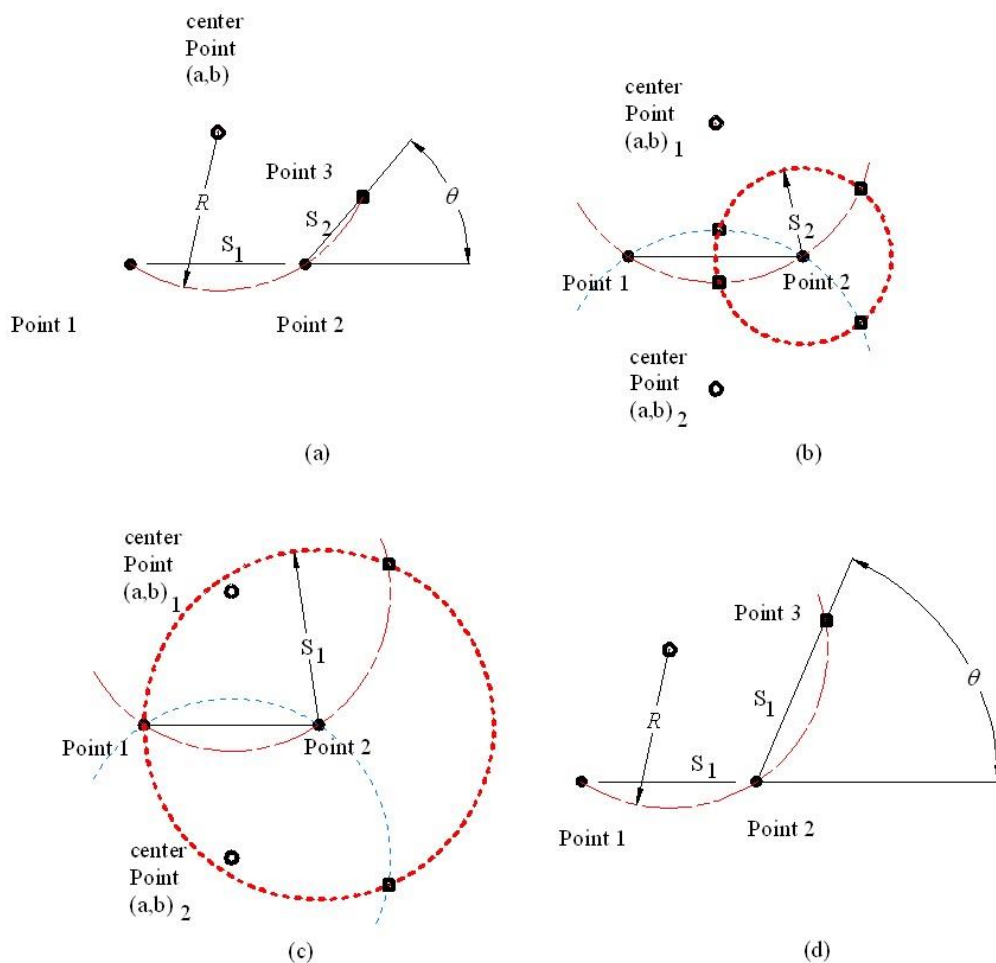

Figure 7. The process of creating the constant curvature segment from (a) through (d).

5.0 SELECTION OF CONSTANT CURVATURE LINKS WITH PRISMATIC JOINTS

In MATLAB, the selection process involves looking at the plot of curvature and point numbers as in Figure 8(a) for example. The less clutter the data distribution gets, the easier it is to see which curvature points could fall under the same band. The band of curvature translate to the range that the points will have rather similar average radius, so that a single radius prismatic link can connect them.

The selection can be done for one prismatic joint or link at a time. Within the closed curvature band, the start point and the stop point of the prismatic link are selected for each profile. After this is done, the plot of the profiles will be updated with all curves beginning at the stop points in the previous selection. Next, if there are points that fall in another band, the same selection process is taken.

Figure 8(b) illustrates this concept. The aim is mainly to get as many links with prismatic joint as possible. However, each prismatic set is to be selected from a band of curvatures that are common throughout all curves involved.

For each link with prismatic joint, the range of point numbers for each target profile can be determined by using the crosshair selection process. From this information the curvature values pertaining to those points, a mean curvature can be calculated. Using the relationship in Equation (6), the mean radius of the constant curvature link with prismatic joint can be found. The prismatic link, whether it is curved or straight, must basically have the same mean radius to operate.

$$r_m = (1/C) \sum_{j=1}^{C} \left((1/n_j) \sum_{i=1}^{n_j} 1/\kappa_{ij} \right) \tag{24}$$

C here is the number of profiles in the synthesis. By knowing this mean radius from Equation (24), next is basically forming an arc with the center at (0,0). The polarity of r_m is important here since it determines the shape of the arc, either concave up or concave down. A negative r_m will start the arc at ($-r_m$, 0) and move clockwise to create concave down shape. On the other hand, a positive r_m will start the arc at (r_m, 0) and move clockwise to create concave up shape.

Each small segment of the arc formed is equal to the size of a mean piecewise linear segment S_m that make up the target profiles. Hence, the formation of the arc occurs at specific delta angle until the range of point numbers selected for a particular prismatic link is covered for that profile. Equation (25) shows how to get the angle.

$$\delta = \cos^{-1}[(S_m^2 - 2r_m^2)/(-2r_m^2)] \tag{25}$$

The step angle δ does not have polarity. The different length arcs are created one for each profile since they have different number of points. Then methods described in section 3 are used to optimally place these arcs back into position. Figure 9 shows the concept for one prismatic link that works on 2 profiles of different length extensions.
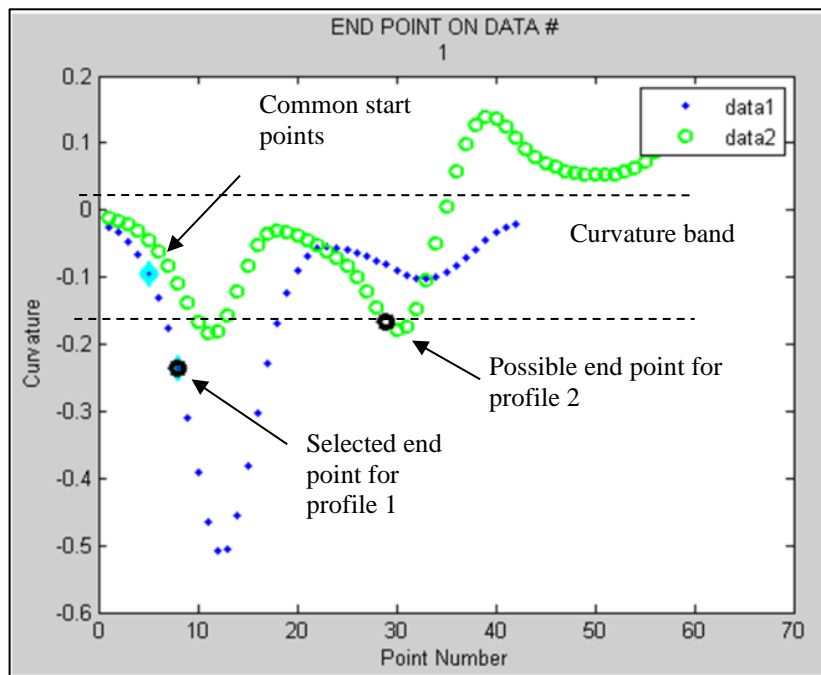
(a)
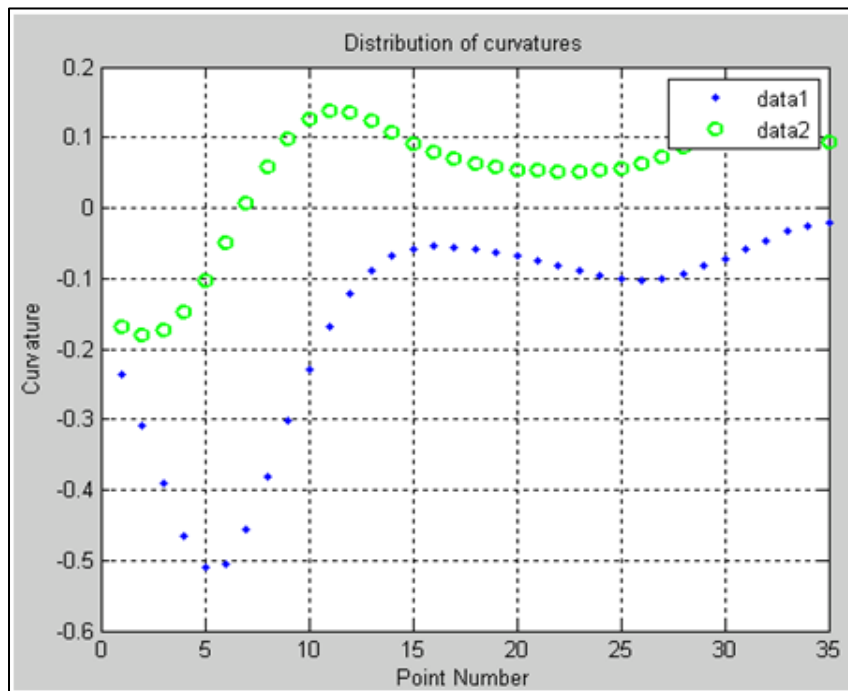
(b)

Figure 8. (a) The curvature band identified for the use of prismatic joint and constant curvature segments. (b) Curvature band left that is suitable for a mean segment. Profiles 1 and 2 relate to data 1 and data2, respectively.
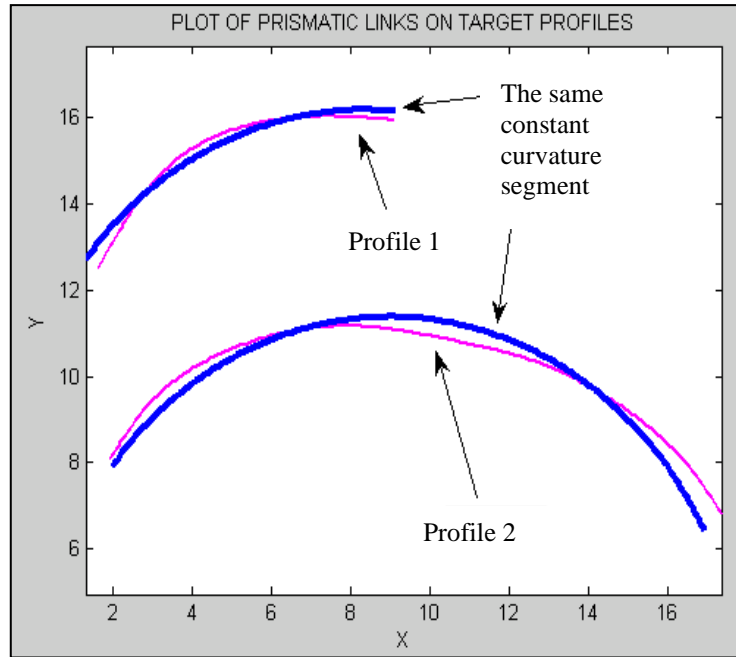
Figure 9. The length-changing link is the same but in two positions.

The next part is filling up the gaps on the profiles that are not specified for prismatic links. Each portion of the gaps must have the same number of points. They each will be filled with one or more rigid bodies until the gaps are filled. The number of rigid bodies used is determined by an error limit set in the program. The motive is to have the rigid bodies to approximate the shape of the profile section that they want to fill.

One would see that the errors after the links or members are connected via revolute joints seem to be higher than they were at segmentation part. The final position of each member is not at optimized minimum distance anymore. Instead, starting from link number 2, each link has to start where the previous link ended. They are connected there. Next, the end of the link points towards the point on each target profile where the link approximates the curve. Therefore, the error of this final position can become significantly higher than before the links are hooked up.

Real world applications include a hull design that would need to change shape in order to obtain the required drag for a craft to move in a fluid. This is depicted by the cross-section of the machine in Figure 10 that may change shape and thus achieving different arc length. Shamsudin in (Shamsudin, 2013) showcased an example of shape-changing slat for a 30P30N airfoil wing. Researchers in (Ismail, Shamsudin & Sudin, 2015) and (Shamsudin & Ismail, 2018) also touched on this novel design of the wing and slat profiles. The paper also suggested some of the benefits especially in terms of lowering noise level. If the airfoil is used underwater, ultrasound can be used to measure fluid velocity around the profiles as in (Daosaeng & Thong-un, 2019). Figure 11 displays a more recent design for the same slat in (Ismail, Shamsudin & Sudin, 2015) where the mechanisms can be simplified further. Some analytical methods in (Myszka, 2009) may help in locating the fixed pivot points in a four-bar mechanism using three-position synthesis. There are various methods – mostly graphical – for this synthesis as explained in enough detail in (Dicker Jr., Pennock & Shigley, 2016), (Myszka, 2015) and (Waldron, Kinzel & Agrawal, 2016).
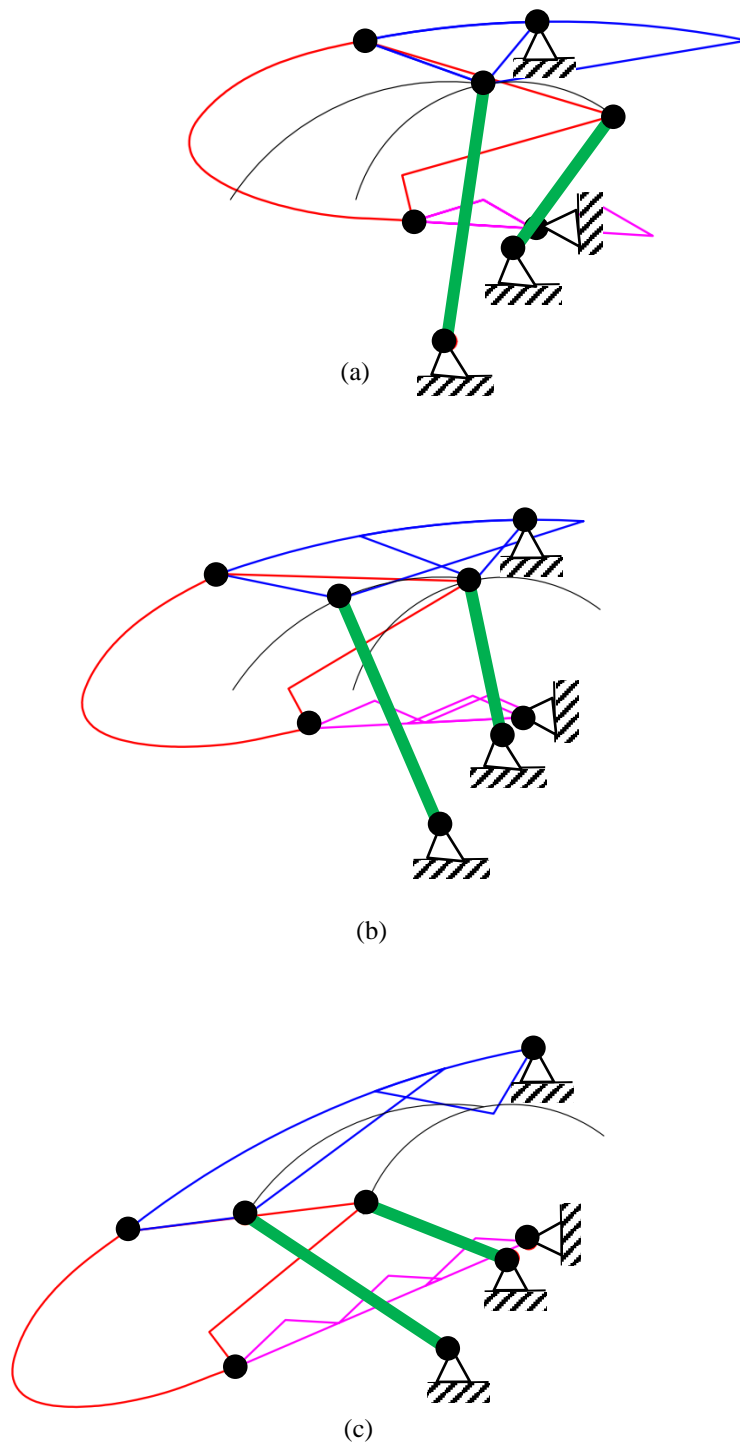
Figure 10. The aircraft wing slat changes between stowed, midway position, and fully deployed as it changes from (a) to (c).

6.0   CONCLUSION

The algorithm being developed here is very promising in approximating the target profiles with links that consist of rigid bodies and prismatic links. The number of rigid bodies that fill the gaps that is not covered by prismatic links can be optimized by using the distances of the mean segment profiles to the target section profiles. The largest distance becomes the error associated with the mean profile. While this error is less than a specified maximum error, such as 0.1, the size of the mean segment profile is increased until its error is just below the maximum error. Then another mean segment is created following the same algorithm until the same-number-of-points section is covered. The overall error will increase though, as the bodies are linked up together with revolute joints.

7.0   ACKNOWLEDGEMENT

8.0   REFERENCES

Daosaeng, J., & Thong-un, N. (2019). A study of flowrate calculation using ESPRIT technique for ultrasonic velocity profiles. *Engineering Journal*, 23(2).

Dicker Jr., J. J., Pennock, G. R., & Shigley, J. E. (2016). *Theory of Machines and Mechanisms* (5th ed.). New York: Oxford.

Ismail, M. H., Shamsudin, S. A., & Sudin, M. N. (2015). Design and analysis of rigid-body shape-change mechanism for aircraft wings. *Jurnal Teknologi*, 77(21), 1-7.

Korte, B. (2006). *The application of rigid-body kinematics to shape-changing mechanism design*. MSc Thesis, The Ohio State University, Ohio, USA.

Lateş, D., Căşvean, M., & Moica, S. (2017). Fabrication Methods of Compliant Mechanisms. *Procedia Engineering*, 181, 221 – 225.

Lobo, P. S., Almeida, J., & Guerreiro, L. (2015). Shape memory alloys behaviour: A review. *Procedia Engineering*, 114, 776 – 783.

Lu, K. J. & Kota, S. (2003). Design of compliant mechanisms for morphing structural shapes. *Journal of Intelligent Material Systems and Structures*, 14, 379 – 391.

Mohd Jani, J., Leary, M., Subic, A., & Gibson, M. A. (2013). A review of shape memory alloy research, applications and opportunities. *Materials and Design*, 56, 1078 – 1113.

Murray, A. P., Schmiedeler, J. P., & Korte, B. (2008). Kinematic Synthesis of Planar, Shape-Changing Rigid-Body Mechanisms. *ASME Journal of Mechanical Design.*130(3), 032302:1–10.

Myszka, D. H. (2009). *Kinematic synthesis and analysis techniques to improve planar rigid-body guidance*. Ph.D. Dissertation, Mechanical & Aerospace Engineering, The University of Dayton, Ohio, USA.

Myszka, D. H. (2015). *Machines and Mechanisms: Applied Kinematic Analysis* (4th ed.). New Jersey: Pearson.

Nespoli, A., Besseghini, S., Pittaccio, S., Villa, E., & Viscuso, S. (2010). The high potential of shape memory alloys in developing miniature mechanical devices: A review on shape memory alloy mini-actuators. *Sensors and Actuators A*, 158, 149–160.

Rubbert, L., Charpentier, I. Henein, S., & Renaud, P. (2017). Higher-order continuation method for the rigid-body kinematic design of compliant mechanisms. *Precision Engineering*, 50, 455–466.

Shamsudin S. A., & Murray, A.P. (2013). A closed-form solution for the similarity transformation parameters of two planar point sets. *Journal of Mechanical Engineering and Technology (JMET)*, 5(1), 59 – 68.

Shamsudin, S. A., Murray, A. P., Myszka, D. H., & Schmiedeler, J. P. (2013). Kinematic synthesis of planar, shape-changing, rigid body mechanisms for design profiles with significant differences in arc length. *Mechanism and Machine Theory*, 70, 425–440.

Shamsudin, S. A. (2013*). Kinematic synthesis of planar, shape-changing rigid body mechanisms for design profiles with significant differences in arc length*. Ph.D. Dissertation, The University of Dayton, Ohio, USA.

Shamsudin S. A., & Ismail, M. H. (2018). The applications of shape-changing rigid body mechanisms in arts and engineering. *Journal of Advanced Manufacturing Technology (JAMT)*, 12-1(2), 301-312.

Trease, B. P., Moon, Y. M., & Kota, S. (2005). Design of Large-Displacement Compliant Joint. *Transaction of the ASME*, 127, 788 – 798.

Waldron, K. J., Kinzel, G. L., & Agrawal, S. K. (2016). *Kinematics, Dynamics, and Design of Machinery*. Sussex, UK: John Wiley.

Weishaar, T. A. (2006). Morphing aircraft technology – new shapes for aircraft design. In *Multifunctional Structures/Integration of Sensors and Antennas Meeting Proceedings. RTO-MP-AVT-141, Neuilly-Sur-Seine, France.*